CONTINENTAL MARGIN SUBSIDENCE AND HEAT FLOW: IMPORTANT PARAMETERS IN FORMATION OF PETROLEUM HYDROCARBONS

by
LEIGH ROYDEN, J. G. SCLATER,
AND R. P. VON HERZEN

Reprinted for private circulation from
THE AMERICAN ASSOCIATION OF PETROLEUM GEOLOGISTS BULLETIN
Vol. 64, No. 2, February, 1980

The American Association of Petroleum Geologists Bulletin
V. 64, No. 2 (February 1980), P. 173-187, 13 Figs. 2 Tables

Continental Margin Subsidence and Heat Flow: Important Parameters in Formation of Petroleum Hydrocarbons[1]

LEIGH ROYDEN,[2] J. G. SCLATER,[3] and R. P. VON HERZEN[4]

Abstract Passive continental margins have been shown to subside with a 50-m.y. exponentially decaying rate which cannot be explained by isostatic compensation for sediment loading. This suggests that the subsidence is dominated by geodynamic processes similar to those in the deep ocean. Two simple geologic models for continental breakup are developed: (1) attenuation of continental lithosphere and (2) intrusion of mantle diapirs.

These models for rifting give a direct relation between subsidence of passive margins and their surface heat flow through time. On this basis we develop a method of reconstructing the thermal history of sedimentary strata from regional subsidence and sedimentation history. Because generation of petroleum hydrocarbons depends on the integrated time/temperature history of buried organic material, this reconstruction technique can be used to determine the depth to the oil range of the "hydrocarbon generation window" in advance of drilling. By way of example, we reconstruct time/temperature/depth plots and estimate hydrocarbon maturity for one site in the Falkland Plateau and three sites in the North Atlantic near Cape Hatteras. In addition to providing a method for evaluating hydrocarbon potential in frontier regions where there is little or no well control, this approach suggests that there may be significant potential for oil and gas generation on the outer part of the continental rise and in deep-sea sedimentary basins.

INTRODUCTION

Variations of heat flow and topography in the ocean floor can be adequately explained as the thermal contraction of a cooling lithosphere (Langseth et al, 1966; Parker and Oldenburg, 1973; Parsons and Sclater, 1977). Parsons and Sclater (1977) considered a simple plate model in which the lithosphere is assumed to be a slab of uniform thickness. Material is intruded at constant temperature along mid-ocean ridges and subsequently spreads away from the ridge axis. The lithosphere is allowed to cool conductively while the lower slab boundary is maintained at the temperature of intrusion, and the ocean floor subsides owing to thermal contraction. Initially, depth increases as the square root of time ($\sqrt{t}$; symbols used in text are defined in Table 1) but for older ocean floor ($t \geq 80$ m.y.) appears to increase at an exponentially decaying rate toward a constant asymptotic value. From observation of seafloor bathymetry Parsons and Sclater (1977) concluded that between 0 and 70 m.y. after intrusion, depth is given by $d(t) = 2{,}500 + 350\ t^{1/2}$m. For older lithosphere the relation becomes $d(t) = 6{,}400 - 3{,}200 \exp(-t/62.8)$. An analogous age relation holds for surface heat flow. Surface measurements in impermeable sedimentary basins, where the heat transfer is entirely by conduction, give average values in agreement with this theoretical model. For oceanic crust younger than about 120 m.y., the heat flow (Q) may be expressed as $Q(t) = 11.3\ t^{1/2}$ cal cm^{-2}sec^{-1}, and for older crust $Q(t) = 0.9 + 1.6 \exp(-t/62.8)$ cal cm^{-2}sec^{-1}.

There is considerable evidence in the sedimentary record from passive continental margins that a significant fraction of margin subsidence cannot be explained entirely by isostatic compensation for sediment loading. Sleep (1971) has shown that subsidence follows an exponential decay with time constant ~50 m.y. across large regions of the continental shelf (Fig. 1). Similar results were obtained by Watts and Ryan (1976) for the Hatteras region and the Gulf of Lyon. The similarity between these subsidence histories and the

[1]Manuscript received, November 6, 1978; accepted, July 24, 1979.

[2]Department of Earth and Planetary Sciences, Massachusetts Institute of Technology, Cambridge, Massachusetts 02139, and Woods Hole Oceanographic Institution, Woods Hole, Massachusetts 02543.

[3]Department of Earth and Planetary Sciences, Massachusetts Institute of Technology, Cambridge, Massachusetts 02139.

[4]Woods Hole Oceanographic Institution, Woods Hole, Massachusetts 02543.

We thank Shell Development Co., Exxon Research and Production Co., and DOBEX International for their interest and encouragement in this research. In particular we are grateful to John T. Smith and Glenn Buckley for their invaluable criticism of the manuscript, and to the many geochemists who generously took time to explain the rudiments of organic metamorphism and petroleum generation.

Most of this research was supported by Grant 04-7-158-44104, NOAA Office of Sea Grant, U.S. Department of Commerce, to the Woods Hole Oceanographic Institution. The thermal analysis of the Falkland Plateau was supported by the Division of Polar Programs.

Article Identification Number
0149-1423/80/B002-0002$03.00/0

Table 1. Symbols and Values Used

Symbol	Value	Definition
α	$3.3 \times 10^{-5\circ}C^{-1}$	Coefficient of thermal expansion
d		Depth below sea level
γ_d		Fraction (by volume) of lithosphere composed of dikes and intrusive bodies
γ_s		Fraction of lithosphere replaced from below by aesthenosphere
γ		Oceanization or thermal parameter; γ=0 is continental lithosphere, γ=1 is oceanic lithosphere.
κ	8×10^{-3} cm^2 sec^{-1}	Thermal diffusivity of lithosphere
K	7.5×10^{-3} cal cm^{-1} sec^{-1} ° C^{-1}	Thermal conductivity of lithosphere
K_{sed}	4×10^{-3} cal cm^{-1} sec^{-1} °C^{-1}	Thermal conductivity of sediment
l	125 km	Equilibrium thickness of lithosphere
$l^2 \kappa/\pi^2$	62.8 m.y.	Time constant of thermal decay
Q		Heat flow
ρ_m	3.33 gm cm^{-3}	Density of mantle
ρ_w	1.0 gm cm^{-3}	Density of water
ρ_c	2.8 gm cm^{-3}	Density of crustal rock
S_i		Initial subsidence due to stretching
t		Time measured in millions of years
t_c		Crustal thickness
T		Temperature
T_m	1,350° C	Temperature of upper mantle
U		Height above equilibrium elevation

depth-age relation for older ocean floor strongly suggests that the subsidence of passive continental margins results from thermal contraction of the lithosphere, and that there may be a simple thermal model to explain the geologic history of some margins. Most recently, Steckler and Watts (1978) have used a thermal model to explain the subsidence observed at the COST B-2 well.

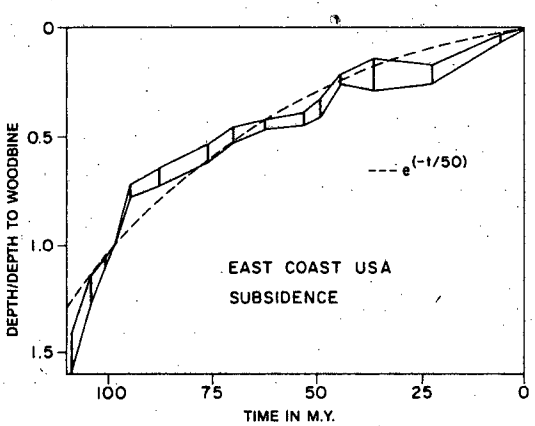

FIG. 1—Depth normalized to base of Woodbine is plotted as function of age for wells on East Coast of United States. Dashed smooth curve is 50-m.y. exponential constrained to fit data at base of Woodbine and at present (after Sleep, 1971).

Early attempts to model passive continental margins (Sleep, 1971) simply considered the continental lithosphere to be heated from below. This produced doming of the lithosphere along the plane of incipient rifting (Fig. 2A), and adequately described the subsidence history of the margin. Two more sophisticated models have been suggested: the first entails rapid stretching and attenuation of the continental lithosphere at the time of continental breakup (Fig. 2B; McKenzie, 1978); the second, a modification of Burke's aulacogen theory (Burke and Whiteman, 1973), involves cracking of the continental lithosphere and large-scale intrusion of diapirs across the incipient margin (Fig. 2C). At present it is not clear which of these mechanisms dominates margin formation; both produce the same subsidence history, but differ radically in estimates of initial heat flow. It seems probable that both mechanisms may be active during continental breakup.

If marginal evolution can be explained by a combination of these mechanisms, the paleoheat

flow must lie within a range bounded by the two extreme models. Thus by correlating subsidence with thermal evolution of sedimentary basins, we can predict a range for paleoheat flow. To reconstruct paleoheat flow for individual basins, the following parameters must be known: regional subsidence, depth to basement, sedimentation history, and sediment density. In addition, if thermal conductivities are known or if they can be estimated from sediment lithology, the thermal history of any sedimentary unit can be traced from the time of its deposition.

SIMPLE RIFTING MODELS

Passive margins may be subdivided into two distinct regions: that part of the margin underlain by oceanic basement, and the region landward from there. For normal ocean floor, the subsidence and heat flow are well determined as a function of age (Fig. 3; Parsons and Sclater,

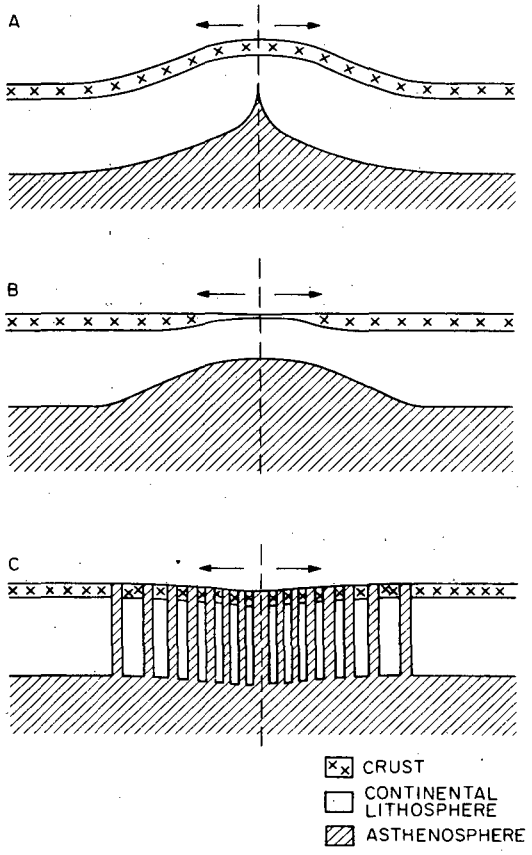

FIG. 2—**A**, In simple rifting model, continental lithosphere is heated along plane of incipient rifting, producing thermal expansion of lithosphere, and doming of surrounding region. **B**, More sophisticated extension model stretches lithosphere across plane of rifting. Hot material rises from asthenosphere to replace thinned continental lithosphere. There is initial subsidence in continental crust as isostatic equilibrium is maintained. **C**, Continental margin is formed by series of ultrabasic dikes intruded across incipient margin. Percentage of dike material increases seaward across margin, with 100% dike material corresponding to pure oceanic lithosphere.

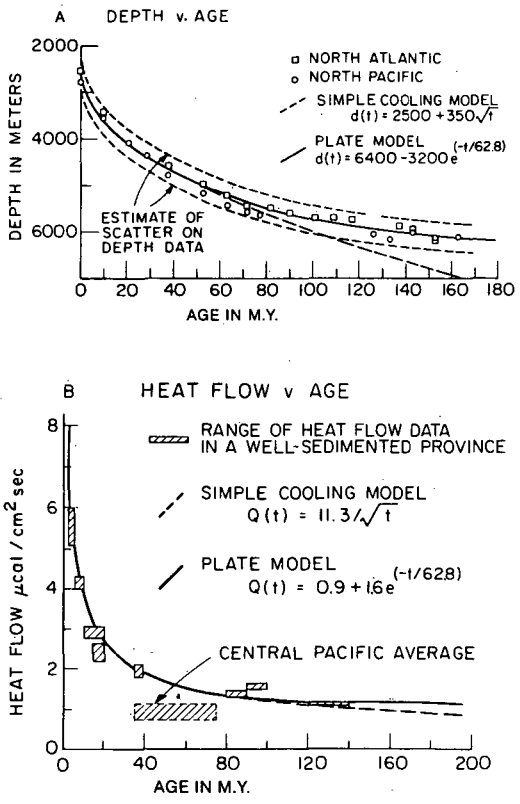

FIG. 3—**A**, Diagram presenting relation between mean depth and age for North Atlantic and North Pacific. Area between short dashed lines represents estimate of scatter in original points used to determine mean data. Solid line beyond 60 m.y. is theoretical elevation from plate model where $d(t) = 6{,}400 - 3{,}200\, e^{-(t/62.8)}$. Line of longer dashes is elevation calculated assuming that lithosphere is simple boundary layer and continues to thicken with time. **B**, Plot of mean heat flow against age. Only values in areas covered by thick layer of sediments are shown. Except for one point in central Pacific there is strong correlation between heat flow and age. Dashed line represents relation between heat flow and age predicted by simple thermal boundary layer model. Heavy continuous line represents relation $Q(t) = 0.9 + 1.6e^{(-t/62.8)}$ predicted by plate model.

1977). Landward of oceanic basement, the situation becomes more complex. We have assumed that margin subsidence can be explained by simple thermal contraction of the lithosphere rather than phase changes in the earth, a process about which little is known. Subsidence and heat flow can then be expressed as the decay of initial thermal conditions toward an equilibrium state, and may be determined by the specific dynamics of margin formation.

Sleep (1971) assumed that the "transitional" part of the margin was continental lithosphere, heated at the time of rifting, and subsequently allowed to cool conductively in the vertical direction, producing subsidence:

$$U(t) = U_o(x)\exp(-at)$$

where $U_o(x)$ is initial uplift and $1/a \sim 50$ m.y. This approach was successful in explaining the general subsidence observed on the East Coast of the United States but encounters substantial quantitative difficulties in some regions. Any region which is uplifted by thermal expansion of the lithosphere will subside to its initial elevation as the lithosphere cools. Consequently, to transform a surface initially at or above sea level into a sedimentary basin (or sedimented margin), the average density of the lithosphere must be increased, either by subaerial erosion, subcrustal thinning, or some other mechanism. Sleep estimated that for an initial uplift of 1.5 km (from sea level), 3.0 km of crust is removed by subaerial erosion and 2.0 km of sediment accumulates in the resulting basin. This result has difficulty in accounting for regions of the East Coast of the United States where thick sediment accumulations of up to 10 km or more overlie continental basement. Sleep's calculations imply removal of $\sim$15 km of crust and an initial uplift of $\sim$7.5 km. There are two problems. (1) Thermal expansion of the lithosphere by 7.5 km is equivalent to raising the temperature to 2,000°C throughout; this is an unlikely supposition, for the base of the lithosphere is generally accepted to remain at about 1,300°C. (2) This model generates huge volumes of terrigenous sediment fairly soon after rifting, but it is difficult to determine where such a large volume of sediment could have been deposited. There is no evidence that it was deposited inland and there does not seem to be enough early sediment accumulation on the continental rise and farther out in the deep ocean to account for an erosional event of this magnitude (E. Uchupi, personal commun.).

Another objection to this simple thermal expansion/contraction mechanism for producing marginal basins is the existence of subsiding sedimentary basins which appear to have had neither uplift nor erosion. Sleep (1971) has shown that several of these basins in North America are subsiding with an exponential decay rate similar to that observed along the East Coast margin. If the mechanism of subsidence in these basins is similar to that along passive margins, uplift and erosion apparently are not an integral part of their evolution. Yet despite these difficulties with this simple thermal model, its success in producing the general subsidence on the East Coast margin strongly indicates that the subsidence for this region is primarily a cooling effect in the lithosphere.

The general problem of excessive uplift can be avoided if there is crustal extension and thinning at the time of rifting (Fig. 4). Such a model was

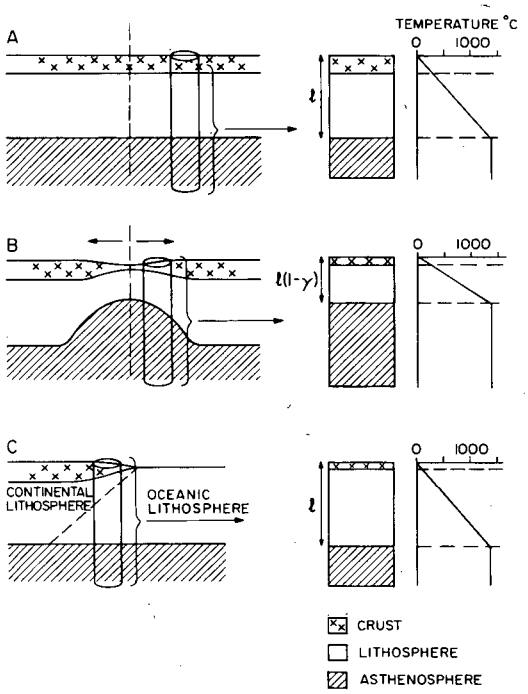

FIG. 4—**A**, Schematic diagram of continental lithosphere prior to initiation of rifting. Temperature profile at right shows lithospheric slab to be at thermal equilibrium with $T_m = 1{,}300$°C at base of lithosphere. **B**, As rifting proceeds, continental lithosphere stretches across plane of rifting, thinning both lithosphere and continental crust. Temperature remains fixed at base of lithosphere, thus steepening thermal gradient. **C**, Long after margin formation, temperature has cooled to equilibrium (Fig. 5A). Margin itself consists of wedge of formerly continental lithosphere which thins seaward (shown by dashed line). Ocean-continent boundary in lithosphere is descriptive only, having no structural significance in old (i.e., cool) margin.

first proposed by Artemyev and Artyushkov (1969) to explain seismic and gravimetric data from Baikal basin. Shallow-angle listric normal faults observed in the Great Basin provide a possible mechanism for stretching and thinning of rigid crustal material (Wright, 1976). These faults, which dip at angles of less than 45°, are associated with steeply tilted blocks. Palinspastic restoration of southern Death Valley indicates that the faulted rock units have been extended by 30 to 50% (Wright and Troxel, 1967). Thinned crust has also been observed under other sedimentary basins (Stegena, 1964; Artemyev and Artyushkov, 1969).

The thermal effects of stretching the lithosphere during margin and basin formation have been explored in detail by McKenzie (1978), where attenuated lithosphere is replaced by passive upwelling of hot asthenosphere. For regions with initial crustal thickness greater than ~20 km, crustal attenuation results in immediate subsidence to maintain isostatic equilibrium. Although there is evidence for some uplift and erosion along passive continental margins, this phenomenon may be due to the introduction of additional heat into the lithosphere which is not directly associated with the thermal effects of lithospheric attenuation. This model is compatible with the observational work done by Sleep and others on margin subsidence. For time greater than ~30 m.y., the subsidence rate is approximately an exponential decay, similar to the exponential subsidence in the deep ocean. The total amount of subsidence is determined by the degree of lithospheric attenuation.

Another model which provides an exponential subsidence compatible with observational data consists of cracking of the continental lithosphere and intrusion of dikes or diapirs from the mantle (Fig. 5). Replacement of light crustal rocks by denser ultrabasic or basaltic material results in initial subsidence and avoids the general problem of uplift. The primary evidence for intrusional activity during margin formation is the extensive dike swarms in east Greenland (Wager, 1947). Other evidence of intrusional activity associated with continental breakup is present in the Lebombo monocline (Cox, 1972) and the Panvel flexure, south of Bombay (Auden, 1972). Whether this intrusional activity is a primary mechanism of margin formation or only an incidental by-product of some other process is unclear. It seems unlikely that this mechanism can be operant at depths where the lithosphere may behave as a viscous fluid rather than a rigid, brittle slab. Nevertheless, the lithosphere possibly extends by ductile flow near its lower boundary and by extensional cracking and dike intrusion in its upper part.

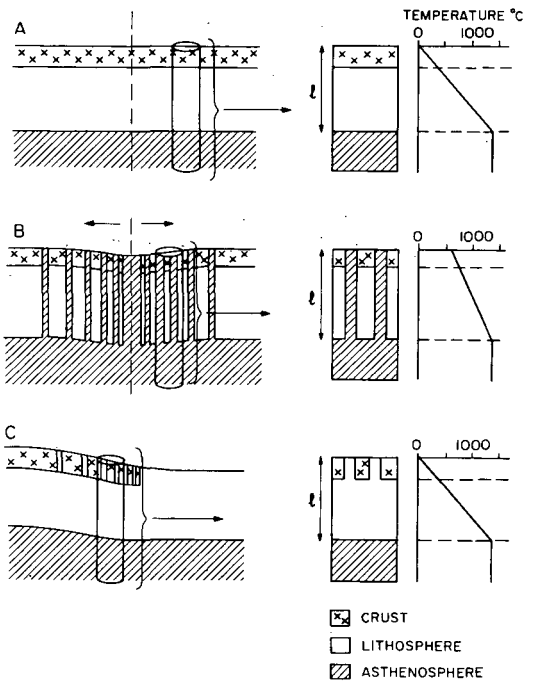

FIG. 5—**A**, Continental lithosphere prior to rifting, as in Figure 4A. **B**, As rifting proceeds, lithosphere cracks and ultrabasic dikes are intruded along plane of rifting. Dikes increase in volume and/or frequency toward axis of rifting. Transition to pure oceanic crust occurs when intruded ultrabasic material becomes 100% of total. Temperature gradient through lithosphere becomes less steep, but surface temperature is raised considerably. **C**, Long after rifting, temperature gradient has returned to equilibrium. Margin consists of continental crust interrupted by series of dikes which may not all reach surface.

DISCUSSION

The theoretical subsidence and heat flow resulting from these models have been calculated mathematically (Appendix) and the results are plotted in Figure 6. The degree of "oceanization" is indicated by a thermal parameter, γ. For both models of rifting, $\gamma = 1$ represents pure oceanic crust and $\gamma = 0$ represents undisturbed continent. Corresponding values of γ reflect the addition of equal amounts of heat to the continental lithosphere at time $t = 0$. Because the system returns to equilibrium at $t \to \infty$, the total subsidence and net heat loss from the lithosphere are a function only of γ, and independent of the model. For equal values of γ, there are slight differences in subsidence versus time for the two models but they do not appear large enough to be distin-

guished from observational data. Likewise, for equal values of γ, the heat flow curves are virtually identical after about 20 m.y., but for $\gamma < 0.6$ there are significant differences in heat flow at times <20 m.y. This is to be expected considering the different initial temperature distribution, particularly in the near-surface region (Figs. 4B, 5B).

Because initial elevation was taken to be at or below sea level, Figures 6A and 6C show both the effect of thermal contraction of the lithosphere and the related effect of isostatic compensation for water loading. Most subsiding sedimentary basins and margins contain large thicknesses of sediment, and regional subsidence must be determined indirectly by examining the time stratigraphy in the sediments and compensating for the effect of sediment loading.

This gives a simple method for calculating a range of paleoheat flow along margins and in basins where the sedimentation history is known. Because theoretical subsidence depends primarily on γ and not on the specific thermal model (Fig. 6A, C), calculation of empirical subsidence yields a unique value for γ. Because we do not know the

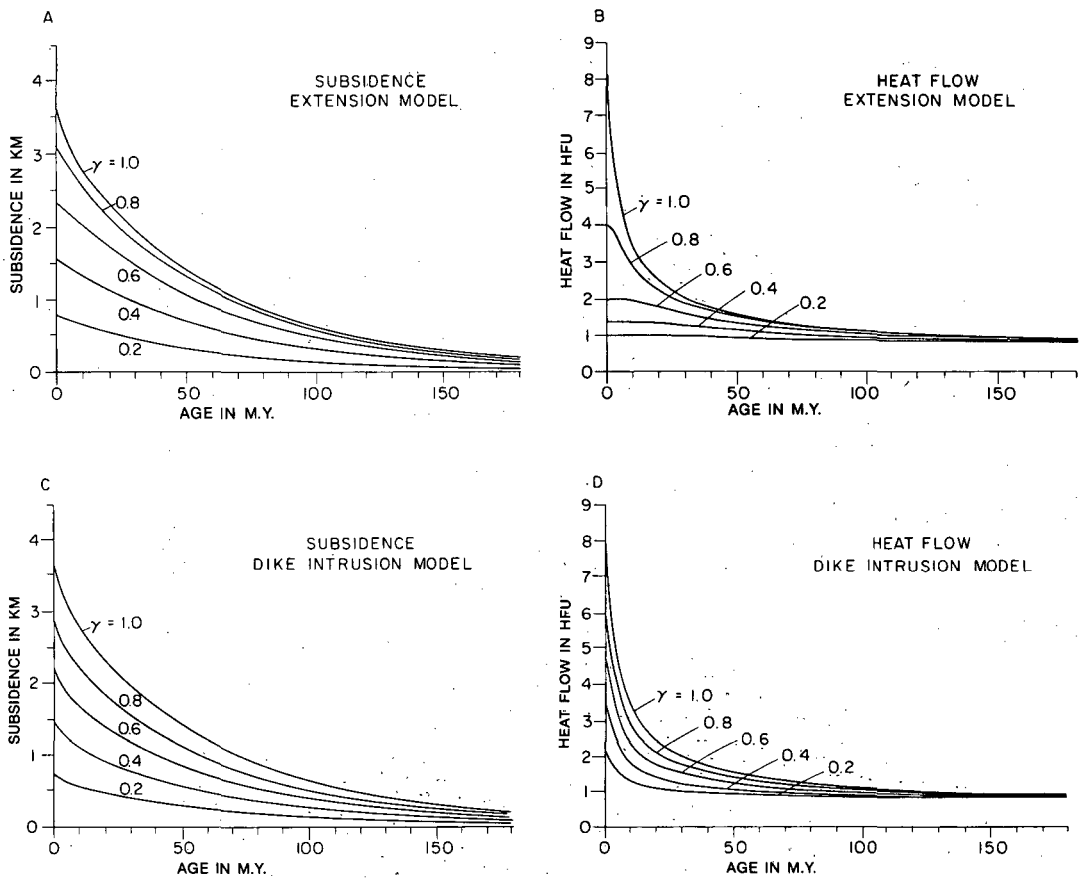

FIG. 6—**A**, Theoretical surface elevation calculated from equation 7a for extensional margin. Curve given by $\gamma = 1$ corresponds to pure oceanic lithosphere and is identical to Figure 4A. For all values of γ, depth approaches constant value. **B**, Theoretical heat flow calculated from equation 6a. Again, $\gamma = 1$ corresponds to pure ocean floor. After about 100 m.y., heat flow becomes 1.0 heat flow unit (HFU) for all values of γ. For $\gamma < 0.6$, initial heat flow is quite low, which results from great depth at which heat is added to lithosphere; the greater the depth, the longer the time until effects are felt at surface. **C**, Theoretical surface elevation calculated from equation 11a; $\gamma = 1$ corresponds to pure oceanic lithosphere, and is identical to curve for $\gamma = 1$ in **A**. For all values of γ in this figure, rate of subsidence is equal to that in deep ocean multiplied by factor of γ, that is $U(t) = \gamma \cdot \Delta E(t)$ where $E(t)$ is surface elevation of oceanic lithosphere. **D**, Theoretical heat flow calculated from equation 10a. High values of initial heat flow reflect addition of heat close to surface.

specific mechanism for margin formation, we cannot reconstruct the heat flow exactly. However, the two models developed previously may be taken as limiting examples and hence we can reasonably expect the paleoheat flow to lie within the bounds set by these two extremes. Because temperature at depth is directly related to heat flow, our thermal models may be used to determine paleotemperatures in specific sedimentary strata and to estimate the thermal potential for petroleum genesis. In near-surface regions heat flux can be considered invariant with depth, and within the sedimentary layer temperature at z_o is given by:

$$T = T_{surface} + \int_0^{z_0} \frac{Q(t)dz}{K(z)}. \quad (1)$$

Equation 1 is a good approximation provided that an equilibrium situation prevails throughout the sedimentary layer, that no heat is derived from radioactive isotopes in the sediment or underlying crust, and that convection of interstitial water provides a negligible contribution to total heat transport. The sedimentary layer should be in thermal equilibrium when the sedimentation rate does not exceed 1 km in a million years. In general, the contribution from radiogenic heat sources is not negligible, and for precise temperature calculations this equation should contain a third term for this. We expect that the two models will produce similar thermal histories for $\gamma = 1.0$ and $\gamma = 0$ but for intermediate values of γ we expect higher temperatures in the dike intrusion model for very early times, and hence more mature hydrocarbons in the early sedimentary series.

Paleoheat flow cannot be measured directly, but there are at least two other tests of these models. We can compare calculated values for heat flux with present-day heat flux in very young sedimentary basins ($\leq$ 10 m.y.), or we can compare them with the extent of thermal alteration of organic material in older sediments as an indication of prior thermal gradients. It would be more straightforward to measure heat flow directly in a young basin, but the subsidence history in such a basin may not be well enough defined to calculate any meaningful value of γ. In the second test, most passive margins are older than about 70 m.y. and may be buried by up to 15 km of sediment. Thermal alteration in the sediments deposited shortly after rifting and during the period of variable heat flow ($<$30 m.y. after rifting) is generally obliterated by the subsequent burial and high-temperature environment. Exceptions are present in regions where considerable thicknesses of pre- and syn-rift sediments have gone through the peak thermal event and been highly altered during the high heat flow phase. Thermal alteration in sediment deposited after this period of variable heat flow is less conclusive, for the heat flow curves become very flat and often indistinguishable. Nevertheless, it is possible to make some gross generalizations about temperature history in older, well-sedimented basins and continental shelves.

For a sedimentary basin filling to sea level, the temperature at the sediment-basement interface is a function of two variables: sedimentary thickness and heat flow. Because the basin fills to sea level, the sedimentation rate is effectively determined by thermal contraction of the lithosphere and hence is directly related to heat flow. It can be shown from the equations derived in the appendix that the temperature at the sediment-basement interface remains relatively constant after about 70 m.y. The temperature variations which may occur after 70 m.y. are primarily determined by regional geologic processes and, to a lesser extent, by the elevation of basement immediately after rifting. These regional processes include development of horst and graben structures, nonuniform sedimentation, and progradation of the margin.

In basins younger than 70 m.y. it is difficult to make a similar generalization about the temperature at the sediment-basement interface because the basement temperature is also more strongly dependent on initial elevation, sediment supply, and other variables. Likewise, in basins which are sediment starved and do not fill to sea level, the sedimentary thickness and the heat flow are not directly related, and the temperature at basement must be calculated formally. In these regions with a more complex thermal environment, this temperature reconstruction technique is particularly useful.

We have applied the technique to (1) the Falkland Plateau, a subsiding sediment-starved basin; (2) the North American continental shelf near Cape Hatteras, an older sediment-filled basin; and (3) a sedimented region well off the continental rise in North America. Using these results in conjunction with a simple model describing the effects of temperature on metamorphism of organic material, we can estimate the depth of the "hydrocarbon window" for these regions. We do not intend to make a realistic assessment of potential for generation of petroleum hydrocarbons but only to illustrate the possible use of this reconstruction technique. The potential for useful hydrocarbons depends on the presence of source rocks and the possibilities for migration and accumulation, factors which are outside of this discussion. One major source of error lies in our assumption of an arbitrary, uniform thermal

conductivity in the sediment. Because temperature at depth varies inversely with conductivity, accurate determination of thermal conductivity is essential to a rigorous application of this method. Furthermore, this method is clearly inappropriate for regions where there is significant transfer of heat by horizontal or vertical migration of fluids.

THERMAL METAMORPHISM OF ORGANIC SEDIMENTS

Petroleum hydrocarbons are formed by thermal alteration of organic-rich sediments during burial. Although many factors contribute to organic metamorphism, the process is primarily dependent on the integrated time/temperature history of the buried organic material (Tissot et al, 1974). Generally, first-order organic reaction rates approximately double for every 10 to 15°C rise in temperature. In particular, Lopatin (1971) and others have concluded experimentally that the reaction rate for thermal alteration of organic sediments doubles for each 10°C increase in temperature. Hood et al (1975) have shown that this elementary approach gives results in excellent agreement with a more theoretical model which assumes that the reaction is first order in temperature and obeys the Arrhenius equation.

On the basis of these observations, we shall use the following relation for calculating the state of thermal alteration where the parameter C increases as the level of thermal alteration increases.

$$C = \ln \int_0^t 2^{T(t)^\circ C/10} dt \qquad (2)$$

where t = time measured in millions of years and T = temperature in degrees Centigrade. Figure 7 shows how C is related to the level of organic metamorphism (LOM; Hood et al, 1975) and to vitrinite reflectance R_o, which is the most universally accepted measure of the level of thermal alteration of organic matter. As noted on this figure, the oil generation process has barely started at $C \cong 10$, and is essentially complete at $C \cong 16$. The gas generation process is essentially complete at $C \cong 20$. The initiation of gas generation is strongly dependent on the type of organic matter and thus has not been shown on the figure.

APPLICATION

Four major steps in calculating degree of thermal alteration from regional subsidence are: (1) compensation for subsidence due to sediment loading; (2) calculation of γ from thermal subsidence of the region, that is, subsidence not due to sediment loading; (3) from γ, determination of heat flux versus time and thus temperature versus time for specific sedimentary strata; and (4) substitution of T(t) into equation 2 yields thermal potential for hydrocarbon maturation.

As mentioned, it is necessary to subtract the component of subsidence due to sediment loading from the total subsidence so that the remaining or "thermal" subsidence can be compared to theoretical subsidence curves (Fig. 6A, C). In this paper we have chosen to consider only the Airy model for regional isostasy partly because the numerical calculations for this model are less complex than those entailed in a flexural model. It may also be argued that the Airy model gives a better approximation of the loading effect for sediments deposited shortly after rifting (less than about 50 m.y.) when the lithosphere is thinner, hotter, and less rigid than older lithosphere which is near thermal equilibrium. Thus we assume that the subsidence of a sediment-loaded plate (U_s) is related to the subsidence of a water-loaded plate (U_w) by:

$$\frac{\rho_m - \rho_s}{\rho_m - \rho_w} U_s = U_w \, . \qquad (3)$$

Once a thermal subsidence curve has been plotted, an appropriate value of γ can be chosen by

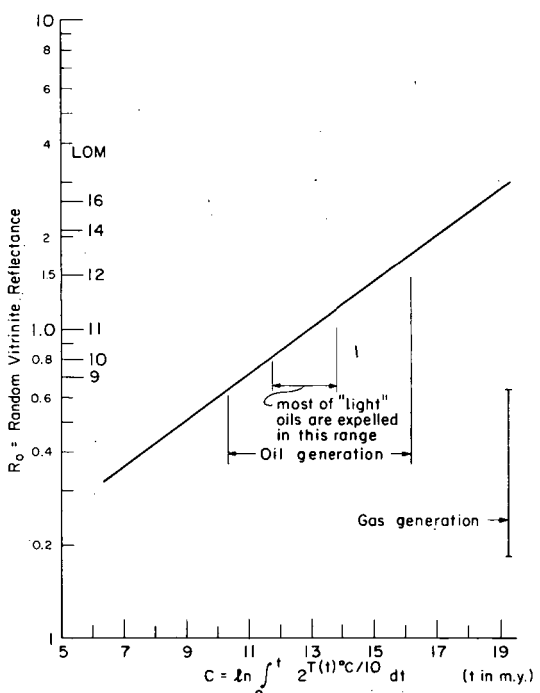

FIG. 7—Plot showing relation of random vitrinite reflectance, LOM, and C. LOM is from Hood et al (1975). Major zones of oil and gas generation are indicated. Start of gas generation is strongly dependent on type of organic material and thus is not shown.

comparison with Figures 6A and 6C. This value of γ can be used to calculate heat flow mathematically, or heat flow may be read directly from Figure 6. This correlation between subsidence history and heat flow is the fundamental step in this reconstruction procedure. Although the mathematical derivation of this may be somewhat complex, the concept is straightforward. This reconstruction technique shows that once heat flow and subsidence have been plotted for a sufficient range of γ, it is unnecessary to recalculate each time the technique is used.

Together with equation 1, this correlation procedure enables us to trace the temperature history of any sedimentary unit where z_o is the depth below the sediment/water interface at any time. Thermal conductivity (K) can be estimated for each lithologic unit in the overlying sediment. Major factors which affect thermal conductivity include sediment composition, porosity, type of interstitial fluid (or gas), and temperature. To avoid the more complex situation of K increasing with compaction and depth of burial, we chose an average value of K and assumed that K remains constant through time. However, it should be strongly emphasized that temperature at depth is directly related to variations in thermal conductivity, and that accurate assessments of conduc-

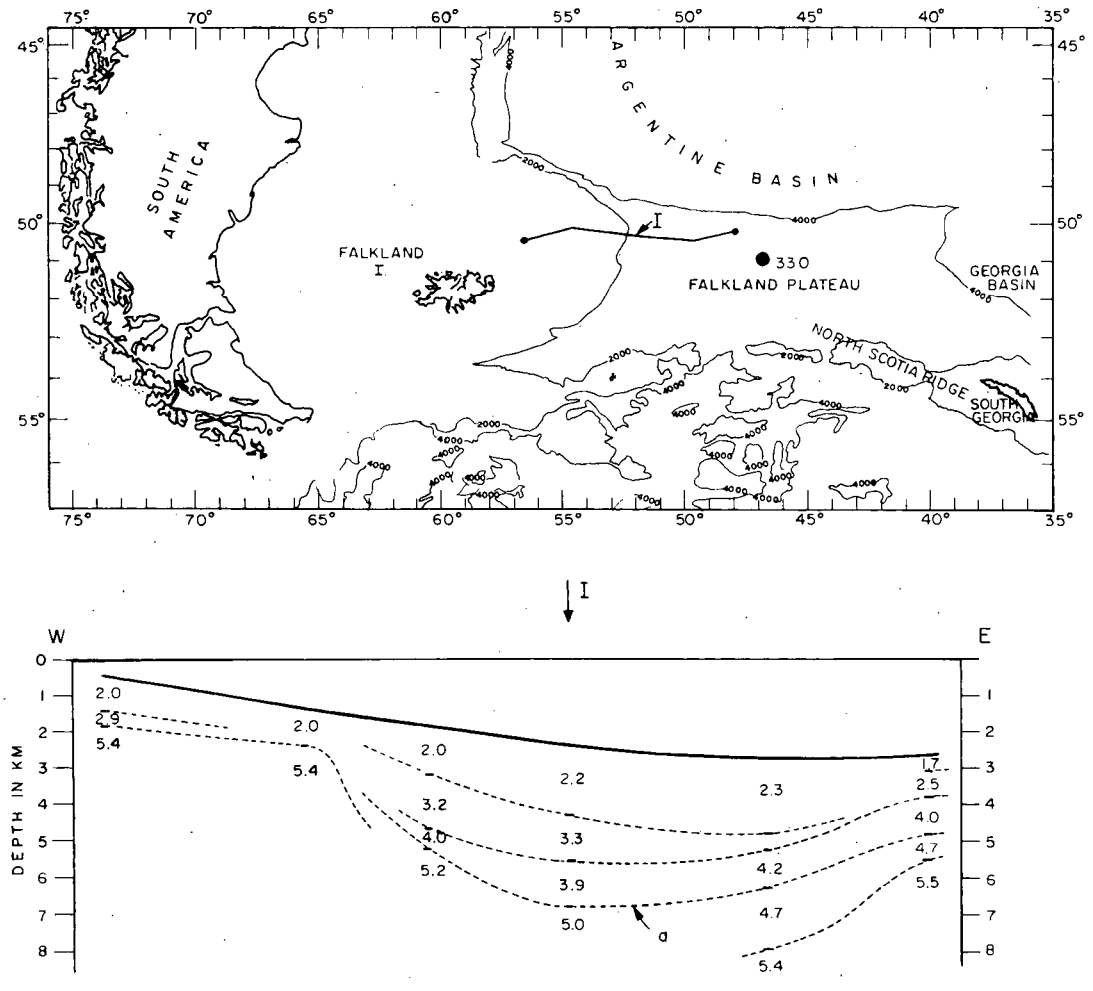

FIG. 8—Location of site I on Falkland Plateau (contours show water depth in meters) and seismic reflection/refraction line (after Ludwig et al, 1979). Reflector *a* is interpreted as pre-Albian depositional hiatus. Figures between dotted lines on section are interval velocities in kilometers/second.

tivity throughout the evolution of the basin are crucial in the application of this technique.

After the temperature history has been calculated for an individual sedimentary package, the stage of thermal alteration (C) can be determined from equation 2 or by any other method which estimates thermal alteration from temperature history. Following are examples in the use of this technique for estimating hydrocarbon potential.

Falkland Plateau

The Falkland Plateau is a sediment-filled basin containing 4 to 5 km of south-dipping sediment. DSDP drilling in the eastern end of the Falkland Plateau has revealed a fairly detailed reconstruction of the post-Paleozoic geologic history, and seismic reflectors can be traced downslope into the major part of the basin (Barker, 1976). Sedimentary records from DSDP Site 330 indicate a marine transgression or minor subsidence event during the Oxfordian. Following this was a depositional hiatus and period of restricted circulation until the end of the Aptian when rapid subsidence established open-marine conditions by early Albian time (Barker et al, 1976). Rapid subsidence during the early Albian can be correlated with the rifting of South America from Africa (van Andel et al, 1977), which strongly suggests that subsidence of the Falkland Plateau is due to thermal effects resulting from continental breakup about 125 m.y. ago. If this is the reason, paleoheat flow and paloetemperature can be reconstructed from the subsidence history of the region.

Figure 8 shows a seismic profile from the central part of the Falkland basin. We have interpreted reflector a as the pre-Albian depositional hiatus and have calculated subsidence history from this horizon. Using density estimates from seismic velocity (Nafe and Drake, 1963), a water-loaded subsidence of 3.5 km (i.e., 3.5 km of subsidence would have occurred without sediment loading) was calculated for basement at site I, roughly corresponding to subsidence of oceanic lithosphere, and suggesting that site I overlies either oceanic basement or transitional basement which is primarily oceanic in character. Assuming a thermal conductivity of $K = 4.0 \times 10^{-3}$ cal cm $^{-1}$ sec $^{-1}$°C^{-1} thoughout the sedimentary layer (King and Simmons, 1972), paleotemperature can be calculated from equation 1. Present-day conductivity for this region is probably closer to 5×10^{-3}, but conductivities in the past must have been considerably lower, for the deeper sediments were initially less compact than at present. Paleotemperature has been superimposed on the sedimentation history of the region and the results are plotted in Figure 9.

Figure 9 shows that the temperature at reflector a has remained relatively constant for the past 80 m.y., whereas temperatures in the overlying sediments have increased somewhat during this time. At no time in the past did these sediments experience temperatures significantly higher than their present temperature. Substitution of temperature versus time into equation 2 for Site I yields the results shown in Table 2. Calculated values of C

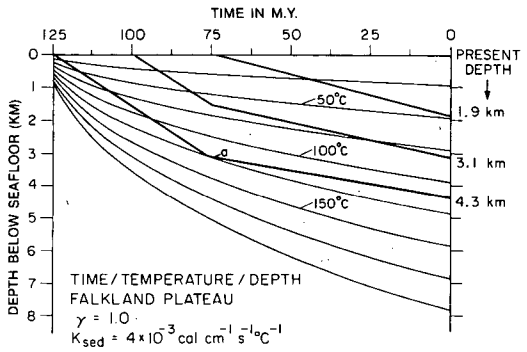

FIG. 9—Time/temperature/depth (TTD) reconstruction for Falkland Plateau at site I. Depth = 0 represents sediment-water interface at all times, and depth is defined as kilometers subbottom. Temperature isotherms, shown by smooth curves, move downward through time, indicating that thermal gradient is becoming less steep. Dark lines represent depositional isochrons, and temperature of specific sedimentary layer can be traced by following appropriate isochron. For example, sedimentary unit deposited at t = 125 m.y. increased rapidly in temperature to 125°C at t = 80 m.y., by which time it had subsided to about 3 km subbottom. At present, that sedimentary unit lies about 4.3 km subbottom and has a temperature of 115°C.

Table 2. Predicted Vitrinite Reflectance

Location (Figs. 8, 10)	Present Depth (km)	Thermal Alteration (C)	Vitrinite Reflectance (Predicted R_o)
Site I	1.9	5.9	x (immature)
	3.1	9.2	0.5
	4.35	12.3	0.9
Site IIa	3.9	9.1	0.5
	5.4	11.9	0.8
	6.9	19.3	x (overly mature)
Site IIb	3.8	7.5 - 9.4	0.4 - 0.5
	6.1	11.8 - 13.0	0.9 - 1.0
Site IIc	3.5	8.2 - 9.4	0.4 - 0.5

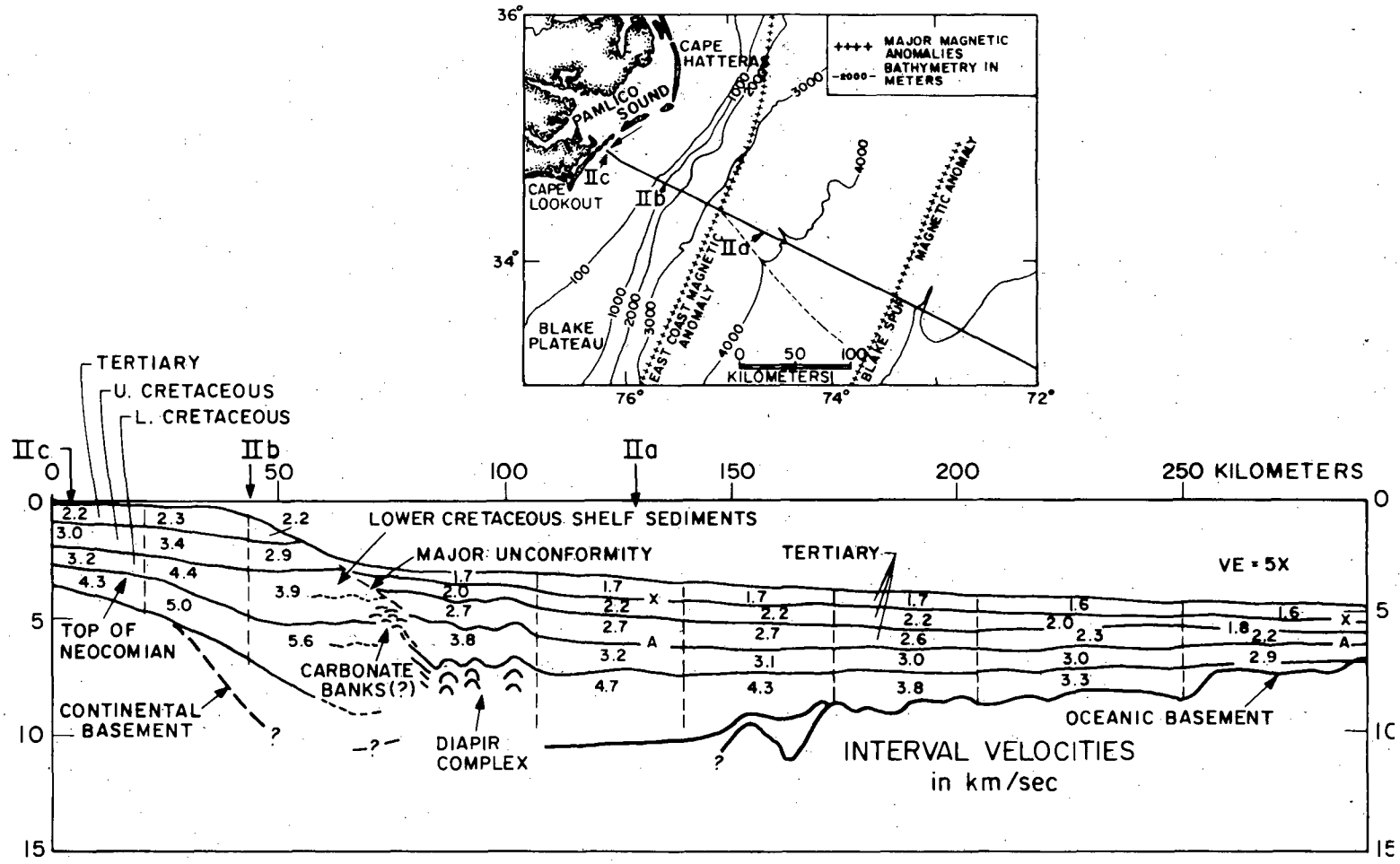

FIG. 10—Seismic refraction line from East Coast continental shelf across Hatteras Abyssal Plain, and location of sites IIa, IIb, and IIc (after Grow and Markl, 1977).

indicate a thermal history compatible with oil generation and possibly gas condensate at depths between 3 and 4.3 km in this part of the Falkland Plateau. However, the presence of oil or gas in this region depends not only upon the thermal history of the area, but also upon sediment composition and structures.

Cape Hatteras: Shelf Region and Abyssal Plain

Figure 10 shows a cross section of the continental shelf near Cape Hatteras and extending across the Hatteras Abyssal Plain. We have chosen three sites, one in the deep ocean (IIa) and two on the shelf (IIb, IIc). Site IIa is almost certainly normal oceanic floor despite the thick sedimentary layer; a significant fraction of this section (layer with interval velocity of 4.7 km/sec) was deposited with 10 m.y. of rifting (Klitgord and Grow, in prep.).

The temperature history of site IIa can be determined by superimposing depositional isochrons onto isotherms calculated from oceanic heat flow. Conductivity of the sedimentary layer has been taken as 4×10^{-3} cal $cm^{-1}sec^{-1}°C^{-1}$, and creation of oceanic basement estimated at 185 m.y. ago.

Figure 11 shows a time/temperature/depth (TTD) plot for site IIa. Early sedimentation caused the temperature at the sediment basement interface to rise to about 250°C. This sediment then cooled to 100°C at 50 m.y.B.P., when an increase in the sedimentation rate again caused a rise in the temperature to its present value of 160°C. Substitution of this temperature history into equation 2 yields the results shown in Table 2 for site IIa. Thermal conditions suitable for oil generation occur at ~4 km depth. This example suggests that there may be oil and gas in other sedimentary basins in the deep sea as well as on the continental rise. On the rise, sediments which were once deeply buried may lie at shallow depth as the result of large-scale erosion coupled with landward retreat of the shelf edge (Grow and Markl, 1977).

Sites IIb and IIc lie on the shelf. Relatively thin initial sediment accumulation suggests that basement was above sea level for a short time after rifting. Estimates of total subsidence from the sedimentation history may be slightly low and hence affect early thermal gradients. Inspection of Figures 12 and 13 shows that this has little effect on the integrated time-temperature history, as early temperatures and sediment accumulation were extremely low.

Subsidence for sites IIb and IIc was corrected to 2.6 and 1.7 km of water-loaded subsidence, corresponding to $\gamma = 0.8$ and $\gamma = 0.5$, respectively. Figures 12 and 13 show TTD plots for both rifting models discussed previously; there is little difference in thermal history produced by each model. Calculation of C and of vitrinite reflectance gives the results shown in Table 2.

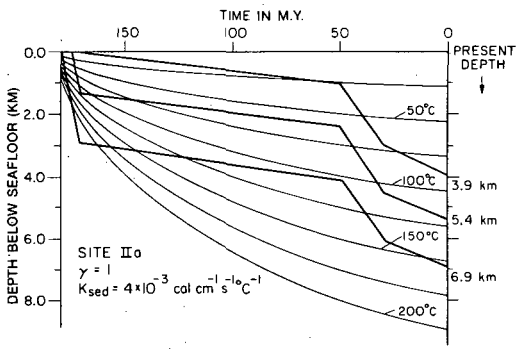

FIG. 11—Time/temperature/depth plot for site IIa on Hatteras Abyssal Plain. Isotherms are calculated from oceanic heat-flow curves and formulae indicated on figure.

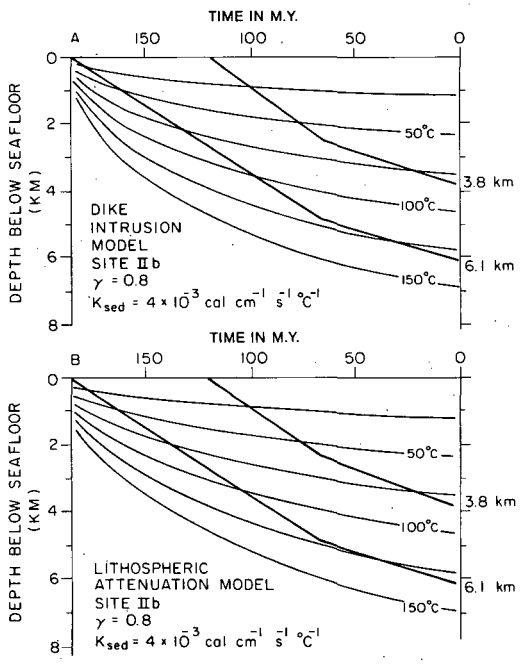

FIG. 12—Time/temperature/depth plot for site IIb on continental rise near Cape Hatteras showing isotherms calculated for two models.

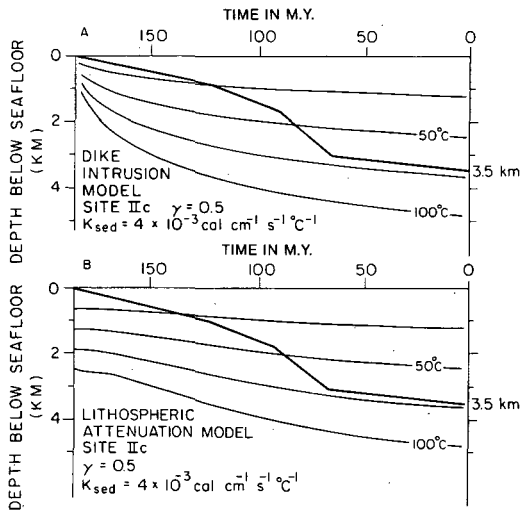

FIG. 13—Time/temperature/depth plot for site IIc showing isotherms calculated for two rifting models.

Higher values of C and R_o are given in each case by the dike intrusion model. Thermal conditions for oil generation begin at about 4 to 5 km depth in site IIb, whereas in site IIc the integrated time/temperature does not appear sufficient for petroleum formation, even at basement.

IMPLICATIONS

The thermal reconstruction technique developed previously is applicable to most passive margins and sedimentary basins formed by thermal contraction and subsidence of the lithosphere, and is a "bare bones" approach to calculating the thermal history of sedimentary sections from their subsidence history. This promises to have immediate application to the evaluation of hydrocarbon potential in frontier areas because, under favorable conditions, the depth of the oil window may be determinable in advance of drilling, or with only sparse well control. More accurate estimates of thermal conductivities in the sediment and of heat supply from radiogenic sources are crucial.

Results from sites IIb and IIc suggest that specific geologic models for rifting may show little difference in temperature history of the sediments unless the sedimentation rate was extremely high just after rifting. Even so, there is little difference in temperature gradient at early times for large values of γ, corresponding to basement which is primarily oceanic in character. This implies that the exact nature of continental breakup may not be determinable from heat flow and subsidence alone because many geologic mechanisms for rifting may yield the observed subsidence and heat flow. Conversely, in most regions hydrocarbon potential may be determined with a fair degree of confidence despite uncertainties about rifting processes.

Perhaps the most interesting application of this model is to starved sedimentary basins where sediment supply was cut off shortly after the peak thermal event. In these regions, sediments which have undergone high thermal gradients associated with basin formation have not been deeply buried by later sedimentation. Consequently, favorable conditions for oil generation are predicted to lie much higher in the sedimentary column than in basins which have filled continuously since initiation of subsidence. In some places, sedimentary sequences on the outer continental rise and just off the rise coincide with this thermal and deposition history.

Prior to 50 m.y. ago, site IIa was a sediment-starved basin comprised of postrifting Jurassic sediments with little or no subsequent accumulation (Fig. 11). This presents a favorable environment for oil generation at shallow depth below the seafloor. If this is a typical deposition pattern for deep-sea basins adjacent to continental margins, many of these basins may also be excellent candidates for oil generation. Although a large pulse of Tertiary sedimentation in the region of site IIa has greatly increased the depth to the hydrocarbon window, this later phase of sedimentation may be missing in other areas. DSDP drilling in the North Atlantic has shown the presence of black shales with organic content in the range conducive to hydrocarbon generation (Lancelot et al, 1972) and sediments containing crude oil have been found in the Caribbean in 3,500 m of water (Davis and Bray, 1969). It seems likely that oil fields in the deep sea may be the next frontier in petroleum exploration.

CONCLUSIONS

1. Two geologic models for rifting, attenuation of continental lithosphere, and injection of mantle material into a series of vertical dikes produce thermal subsidence compatible with observational data for North America. For margins older than 60 m.y., subsidence rate is approximately an exponential decay with time constant ~60 m.y.

2. Heat flux versus time is directly linked with thermal subsidence, that is, subsidence not due to sediment loading. If subsidence and sedimentation history are well known, and estimates of thermal conductivity can be made throughout the section, temperature versus time for individual

sedimentary units can be calculated directly from the regional subsidence history.

3. Most time/temperature reconstructions are not strongly dependent on the exact mechanism of continental breakup, providing that the thermal regime is dominated by simple thermal expansion/contraction of the lithosphere. Exceptions may occur when there are considerable thicknesses of pre- and syn-rifting sediments.

4. Both heat-flow and subsidence curves are fairly flat for margins older than about 70 m.y., and, in basins which fill continuously to sea level, the sediment-basement interface tends toward a constant temperature. However, for very young margins and young sedimentary basins, temperature may vary rapidly with time and cannot be assumed to have remained constant.

5. Used in conjunction with a model which relates level of organic metamorphism to temperature history of organic material, time/temperature/depth reconstructions can determine the thermal potential for organic metamorphism in individual sedimentary units. These reconstructions have immediate application to petroleum exploration because frontier regions could be evaluated for hydrocarbon potential in advance of drilling.

6. This approach suggests that sediment-starved basins, where sediment supply was cut off shortly after the peak thermal event, are a particularly favorable environment for oil and gas generation. In particular, there may be significant potential for petroleum formation in deep-sea sedimentary basins adjacent to the continental rise.

APPENDIX

Thermal Models

1. *Crustal attenuation and stretching of continental lithosphere* — This model, discussed in detail by McKenzie (1978), is illustrated in Figure 4. At $t=0$, the time of rifting, the continental lithosphere is stretched rapidly in the horizontal direction, causing effective thinning of the lithosphere from thickness ℓ to $\ell(1-\gamma_s)$. Isostatic compensation is maintained by upwelling of the hot asthenosphere, which then cools conductively, causing subsidence until thermal equilibrium is reached.

We have assumed throughout that the lithosphere is a slab of thickness ℓ with constant temperature T_m at the base and that the system at all times remains in isostatic equilibrium. The surface of the continent is taken to be at or below sea level so that water occupies the entire volume created by subsidence. We have ignored contributions from radioactivity of crustal rocks, and have neglected two-dimensional effects for the sake of clarity and simplicity. The contribution of sediment loading to overall subsidence has been discussed. Physical parameters are shown in Table 1.

There is an initial change in elevation associated with stretching (McKenzie, 1978, equation 1):

$$S_i = \frac{-\ell\gamma_s[(\rho_m-\rho_c)(t_c/\ell)(1-\alpha T_m t_c/\ell) - \alpha T_m \rho_m/2]}{\rho_m(1-\alpha T_m)-\rho_w}, \quad (1a)$$

where t_c is the initial crustal thickness, α is the coefficient of thermal expansion, and ρ_m, ρ_c, and ρ_w are the densities of the mantle, the continental crust, and seawater, respectively. For the parameters in Table 1, S_i will be negative for regions with $t_c \geq 18$ km, and these areas will show an initial decrease in surface elevation due to stretching.

At time $t=0$, the temperature distribution is:

$$\begin{aligned} T &= T_m, \quad 0 < z/\ell < \gamma_s, \\ T &= T_m\left(\frac{1}{1-\gamma_s}\right)(1-z/\ell), \quad \gamma_s < z/\ell < 1 . \end{aligned} \quad (2a)$$

where z is measured upward from the original lithosphere/asthenosphere boundary.

Maintaining boundary conditions:

$$\begin{aligned} T &= 0, \quad z = \ell, \\ T &= T_m, \quad z = 0, \end{aligned} \quad (3a)$$

we must solve the one-dimensional heat conduction equation:

$$\frac{\partial^2 T}{\partial z^2} = \frac{1}{\kappa}\frac{\partial T}{\partial t}, \quad (4a)$$

where κ is the thermal diffusivity of the lithosphere. The solution for T is (Carslaw and Jaeger, 1959, p. 94):

$$\frac{T}{T_m} = 1 - z/\ell + \frac{2}{\pi}\sum_{n=1}^{\infty}\frac{(-1)^{n+1}}{n}\frac{\sin n\pi(1-\gamma_s)\sin\frac{n\pi z}{\ell}}{n\pi(1-\gamma_s)} \exp(-n^2\pi^2\kappa t/\ell^2) \quad (5a)$$

Solving for the surface heat flux we find

$$Q(t) = -K\left[\frac{\partial T(z,t)}{\partial z}\right]_{z=0}$$

$$= \frac{KT_m}{\ell}\left(1 + 2\sum_{n=1}^{\infty}\frac{\sin n\pi(1-\gamma_s)}{n(1-\gamma_s)}\exp(-n^2\pi^2\kappa t/\ell^2)\right), \quad (6a)$$

where K is the thermal conductivity. The surface elevation is given by:

$$U(t) = \frac{\alpha\rho_m}{\rho_m-\rho_w}\left[\int_0^{\ell} T dz|_{t=t} - \int_0^{\ell} T dz|_{t\to\infty}\right]$$

$$= \frac{\alpha\ell\rho_m T_m}{\rho_m-\rho_w}\left(\frac{4}{\pi^2} - \sum_{m=0}^{\infty}\frac{1}{(2m+1)^2}\left[\frac{\sin[(2m+1)\pi(1-\gamma_s)]}{(2m+1)\pi(1-\gamma_s)}\right]\right.$$

$$\left.\exp(-(2m+1)^2\pi^2\kappa t/\ell^2)\right), \quad (7a)$$

where U(t) is height above final depth as $t\to\infty$. Subsidence and heat flow results are summarized in Figure 6.

2. *Large-scale dike intrusion* — This model is illustrated in Figure 5. At time $t=0$, hot material from the asthenosphere is intruded into the continental lithosphere through a series of vertical dikes. Exposed dike swarms in east Greenland (Wager, 1947) indicate that the density of the intrusions ranges from 5 to 10 per km to 50+ per km. Even if dikes were present only at a spacing of 5 km, the thermal effects of intrusion are averaged horizontally within 1 m.y., which allows us to neglect the horizontal component of heat conduction and consider only a simple one-dimensional problem.

Letting γ_d be the fraction of the lithosphere which is composed of dike material intruded from the asthenosphere, the initial temperature distribution is:

$$T = (1-\gamma_d)(1-z/\ell)T_m + \gamma_d T_m \quad 0 < z/\ell < 1 , \qquad (8a)$$

where z is measured as before. As in the previous model

$$\begin{aligned} T &= 0, \quad & z &= \ell, \\ T &= T_m, & z &= 0, \end{aligned} \qquad (3a)$$

and

$$\frac{\partial^2 T}{\partial z^2} = \frac{1}{\kappa}\frac{\partial T}{\partial t}, \qquad (4a)$$

the solution for T is given by

$$\frac{T}{T_m} = 1 - z/\ell + \frac{2\gamma_d}{\pi}\sum_{n=1}^{\infty}\frac{(-1)^{n+1}}{n}\sin\frac{n\pi z}{\ell}\exp(-n^2\pi\kappa t/\ell^2). \qquad (9a)$$

Likewise the heat flow and surface elevation are respectively:

$$Q(t) = \frac{T_m K}{\ell}(1 + 2\gamma_d \sum_{n=1}^{\infty}\exp(-n^2\pi^2\kappa t/\ell^2)) , \qquad (10a)$$

$$U(t) = \frac{\alpha\ell\rho_m T_m}{\rho_w - \rho_w}\frac{4\gamma_d}{\pi^2}\sum_{m=0}^{\infty}\frac{1}{(2m+1)^2}\exp(-(2m+1)^2\pi^2\kappa t/\ell^2) . \qquad (11a)$$

Results are plotted in Figure 6.

REFERENCES CITED

Artemyev, M., and Ye. Artyushkov, 1969, Origin of rift basins: Internat. Geol. Rev., English Trans., v. 11, p. 582-593.

Auden, J. B., 1972, *in discussion of* K. G. Cox, The Karoo volcanic cycle: Geol. Soc. London Jour., v. 128, p. 334-335.

Barker, P. F., 1976, Underway geophysical observations: Initial Repts. Deep Sea Drilling Project, v. 36, p. 945-970.

——— et al, 1976, Initial reports of the Deep Sea Drilling Project, v. 36: Washington, D.C., U.S. Govt. Printing Office, 1080 p.

Burke, K., and A. J. Whiteman, 1973, Uplift, rifting and the breakup of Africa, *in* Implications of continental drift to the earth sciences, v. 12, pt. 7, Rifts and oceans: London, Academic Press, p. 735-755.

Carslaw, H. S., and J. C. Jaeger, 1959, Conduction of heat in solids: Oxford, Clarendon Press, 496 p.

Cox, K. G., 1972, The Karoo volcanic cycle: Geol. Soc. London Jour., v. 128, p. 311-333.

Davis, J. B., and E. E. Bray, 1969, Analysis of oil and cap rock from Challenger (Sigsbee) Knoll: Initial Repts. Deep Sea Drilling Project, v. 1, p. 415-500.

Grow, J. A., and R. G. Markl, 1977, IPOD-USGS multichannel seismic reflection profile from Cape Hatteras to the mid-Altantic Ridge: Geology, v. 5, p. 625-630.

Hood, A., C. C. M. Gutjahr, and R. L. Heacock, 1975, Organic metamorphism and the generation of petroleum: AAPG Bull., v. 59, p. 986-996.

King, W., and G. Simmons, 1972, Heat flow near Orlando, Florida, and Uvalde, Texas, determined from well cuttings: Geothermics, v. 1, p. 133-139.

Klitgord, K. D., and J. A. Grow, in prep., Jurassic stratigraphy and basement structure of the western Atlantic magnetic quiet zone.

Lancelot, Y., J. C. Hathaway, and C. D. Hollister, 1972, Lithology of sediments from the western North Atlantic, Leg II: Initial Repts. Deep Sea Drilling Project, v. 2, p. 901-949.

Langseth, M. G., X. Le Pichon, and M. Ewing, 1966, Crustal structure of mid-ocean ridges: Jour. Geophys. Research, v. 71, p. 5321-5355.

Lopatin, N. V., 1971, Temperatur a i geologicheskoye uremya kak faktory uglefikatsii: Akad. Nauk SSSR Izv. Ser. Geol., no. 3, p. 95-106.

Ludwig, W. J., et al, 1979, Structure of Falkland Plateau and offshore Tierra del Fuego, Argentina, *in* Geological and geophysical investigations of continental margins: AAPG Mem. 29, p. 125-137.

McKenzie, D., 1978, Some remarks on the development of sedimentary basins: Earth and Planetary Sci. Letters, v. 40, p. 25-32.

Nafe, J. E., and C. L. Drake, 1963, Physical properties of marine sediments, *in* M. N. Hill, ed. The sea, v. 3: New York, Interscience Pub., p. 784-815.

Parker, R. L., and D. W. Oldenburg, 1973, Thermal model of ocean ridges: Nature, Phys. Sci., v. 242, p. 137-139.

Parsons, B., and J. G. Sclater, 1977, An analysis of the variation of ocean floor bathymetry and heat flow with age: Jour. Geophys. Research, v. 82, p. 802-825.

Sleep, N. H., 1971, Thermal effects of the formation of Atlantic continental margins by continental breakup: Royal Astron. Soc. Geophys. Jour., v. 24, p. 325-350.

Steckler, M. S., and A. B. Watts, 1978, Subsidence of the Atlantic-type continental margin off New York: Earth and Planetary Sci. Letters, v. 41, p. 1-13.

Stegena, L., 1964, The structure of the earth's crust in Hungary: Acta Geol. Hungary, v. 8, p. 413-431.

Tissot, B., et al, 1974, Influence of nature and diagenesis of organic matter in formation of petroleum: AAPG Bull., v. 58, p. 499-506.

van Andel, T. H., et al, 1977, Depositional history of the South Atlantic Ocean during the last 125 million years: Jour. Geology, v. 85, p. 651-698.

Wager, L. R., 1947, Geological investigations in East Greenland, pt. IV: Medd. om Grønland, v. 134, p. 1-64.

Watts, A. B., and W. B. F. Ryan, 1976, Flexure of the lithosphere and continental margin basins: Tectonophysics, v. 36, p. 25-44.

Wright, L. A., 1976, Late Cenozoic fault patterns and stress fields in the Great Basin and westward displacement of the Sierra Nevada block: Geology, v. 4, p. 489-494.

——— and B. W. Troxel, 1967, Limitations on right-lateral strike-slip displacement, Death Valley and Furnace Creek fault zones, California: Geol. Soc. America Bull., v. 78, p. 933-958.